by de Gennes.[14]

The effect of polydispersity was discussed in Doi–Edwards' stress relaxation analysis.[3] Here, since the orientation relaxation is explained in terms of the fraction of initial tubes remaining, a similar analyses can be used. Let $P(M)$ be the molecular weight distribution and M_i and M_f be the limits of the distribution. Since in the present theory no interchain correlation is taken into account, each chain contributes to the orientation additively. Therefore, the average fraction of initial tubes remaining at time t can be expressed as

$$\langle F(t) \rangle = \int_{M_i}^{M_f} F_0(t) P(M)\, dM \qquad (14)$$

where $F_0(t)$ is the fraction of the chain remaining inside the initial tubes at time t for the idealized δ-function distribution of molecular weight as expressed in eq 8.

Since the molecular weight dependence of the normalized Hermans orientation function is strong, the effect of polydispersity would be significant even if the sample is nearly monodisperse.

To summarize this FT-IR study, we have concluded that (1) the stages of orientation relaxation can be characterized by using the evaporation of the tube from the initial non-Gaussian conformation to the final Gaussian conformation. This is achieved by the emergence and growth of the minor chain. (2) The scaling arguments seem to be supported by the experimental observations, but further work is needed to explain all the observations.

Acknowledgment. We are grateful to the National Science Foundation for the financial support of this work, Grant DMR 82-16181 (Polymers Program). Appreciation is also expressed to Brian Joss of the Materials Research Laboratory for his assistance in the preparation of the samples and to MRL for its support of the FTIR Facility, NSF-DMR-83-16981.

Registry No. Polystyrene, 9003-53-6.

References and Notes

(1) de Gennes, P. G. *J. Chem. Phys.* **1971**, *55*, 572.
(2) Edwards, S. F. *Proc. Phys. Soc., London* **1967**, *92*, 9.
(3) Doi, M.; Edwards, S. F. *J. Chem. Soc., Faraday Trans. 2* **1978**, *74*, 1789, 1802, 1818; **1978**, *75*, 32.
(4) de Gennes, P. G.; Leger, L. *Annu. Rev. Phys. Chem.* **1982**, *33*, 49.
(5) Kim, Y. H.; Wool, R. P. *Macromolecules* **1983**, *16*, 1115.
(6) Wool, R. P. *J. Elastomers Plast.* **1985**, *17*, 106.
(7) Graessley, W. W. *Adv. Polym. Sci.* **1982**, *47*, 67.
(8) Marrucci, G. *J. Polym. Sci., Polym. Phys. Ed.* **1985**, *23*, 159.
(9) Gaylord, R. J.; DiMarzio, E. A.; Lee, A.; Weiss, G. H. *Polym. Comm.* **1985**, *26*, 337.
(10) de Gennes, P. G. "Scaling Concepts of Polymer Physics"; Cornell University Press: Ithaca, NY, 1978.
(11) Fraser, P. D. B. *J. Chem. Phys.* **1953**, *21*, 1511.
(12) Hermans, J. J.; Hermans, P. H.; Vermaas, D.; Weidinger, A. *Recl. Trav. Chim. Pays-Bas* **1946**, *65*, 427.
(13) Jasse, B.; Koenig, J. L. *J. Polym. Sci., Polym. Phys. Ed.* **1979**, *17*, 799.
(14) de Gennes, P. G. *J. Phys.* **1975**, *36*, 1199.
(15) Boue, F.; Nierlich, M.; Jannink, G.; Ball, R. *J. Phys.* **1982**, *43*, 137.
(16) Narkis, M.; Hopkins, I. L.; Tobolsky, A. V. *Polym. Eng. Sci.* **1970**, *10*, 66.
(17) Cotton, J. P.; Decker, D.; Benoit, H.; Farnoux, B.; Higgins, J.; Jannink, G.; Ober, R.; Picot, C.; Des Cloizeaux, J. *Macromolecules* **1974**, *7*, 863.
(18) Plazek, J. D. *J. Phys. Chem.* **1965**, *69*, 95.

Surface Structure of Segmented Poly(ether urethanes) and Poly(ether urethane ureas) with Various Perfluoro Chain Extenders. An X-ray Photoelectron Spectroscopic Investigation

Sung Chul Yoon and Buddy D. Ratner*

National ESCA and Surface Analysis Center for Biomedical Problems, Center for Bioengineering and Department of Chemical Engineering, BF-10, University of Washington, Seattle, Washington 98195. *Received July 23, 1985*

ABSTRACT: Fluorine-containing segmented poly(ether urethanes) and poly(ether urethane ureas) based on 4,4′-methylenebis(phenylene isocyanate) (MDI) were synthesized by using 2,2,3,3-tetrafluoro-1,4-butanediol (FB), 2,2,3,3,4,4-hexafluoro-1,5-pentanediol (FP), 1,4-diaminotetrafluorobenzene (TFB), or 4,4′-diaminooctafluorobiphenyl (OFB) as chain extenders. The soft segment consisted of poly(tetramethylene glycol) (PTMO) of molecular weight 1000 or 2000. The characterization of polymers was carried out by bulk elemental analysis, gel permeation chromatography, infrared spectroscopy, and X-ray photoelectron spectroscopy (XPS). For the PTMO-2000-containing polymers, the angular dependence of the XPS signal demonstrated that the fluorine content decreases monotonically as one samples closer to the surface and approaches 80–100% of the bulk value at the maximum effective sampling depth (~100 Å). The FB chain-extended polymers have more soft segment at the surface than the FP chain-extended polymers at the same hard-segment content. A decrease in the soft-segment molecular weight from 2000 to 1000 produces an increase of fluorine content or hard-segment concentration in the surface region at the same level of hard-segment concentration. The FP chain-extended polymers based on PTMO-1000 show no angular dependence and have the same fluorine content uniformly distributed throughout the surface region and in the bulk. All of the XPS angular-dependent data indicate that the surface topography of segmented polyurethanes and poly(urethane ureas) strongly depends on the extent of phase separation.

Introduction

Although segmented polyurethanes represent an industrially important class of polymers and their bulk structure and mechanical properties have been extensively studied, the surface structure of these materials has been studied primarily in connection with their application in medical devices. In particular, it has been demonstrated that measurements of the surface composition of these polymers can be correlated with blood interactions.[1,2]

* To whom correspondence should be addressed

0024-9297/86/2219-1068$01.50/0

Thus, if the surface properties of polyurethanes could be precisely controlled, it might be possible to engineer polymers that demonstrate enhanced blood compatibility. In addition, better control of adhesive interactions between polyurethanes and other substrates might be achieved through a better understanding of the polyurethane surface structure.[3-5] To clarify the relationships between the bulk and surface structures for this class of polymers provided the impetus for the studies described here.

The phase separation at polyurethane surfaces is also considered in this study. Many publications have suggested that the extent of domain formation at polyurethane surfaces will strongly influence cell adhesion, protein adsorption, and blood compatibility.[6-11] However, it is not clear that two polymer domains, each with different surface energies, could simultaneously exist at the surface of a polymer.[12,13] The study presented here can provide information on surface phase segregation. This information can be used to construct a picture of the surface structure (in contrast to the bulk structure) of domain-forming segmented polymers. This study can also suggest meaningful model systems that might be synthesized to assess the effect of these surface structures on biological interactions.

Morphologic analyses of segmented polyurethanes or poly(urethane ureas) have shown that these polymers separate into two phases: hard domains, composed of aromatic urethane or urea segments, and soft domains, composed of aliphatic polyether or polyester segments.[14,15] The extent of phase separation of the domains depends on compositional variables such as the symmetry of aromatic diisocyanate,[16] the type of chain extender (diamine or diol),[16-18] the number of carbons in linear low molecular weight chain extenders,[18-22] the type of soft segments (polyether or polyester),[23,24] and the chain lengths of these soft segments.[16,25,26]

If there are two or more block components of different polarity and configuration in a covalently linked block system, there might occur an enriching phenomenon of certain components at the surface. The enrichment at the surface can be governed by the bulk structure, the extent of phase separation near the surface, and/or the surface free energy difference between the two components. Such effects were experimentally confirmed in thorough studies of some di- and triblock copolymer systems, using the X-ray photoelectron spectroscopic (XPS) technique.[27-29] But there are no equally detailed studies for the surface topography of multiblock systems which have a wide distribution of block lengths such as segmented polyurethanes.

In this study, the XPS angular-dependent technique[30] was used to characterize the surface topography/bulk structure relationship for segmented polyurethanes and poly(urethane ureas). Polymer samples used in this type of study must be free of low molecular weight (<5000) components that can potentially dominate the surface structure.[31-33] Finally, the surfaces must be very smooth. If these conditions are met, the angular-dependent XPS technique can be used to generate meaningful depth profile data.

If an XPS angular-dependent study of a diamine-chain-extended segmented polyurethane is performed, the use of the N_{1s} signal can give inaccurate and artifactual results because of its low intensity and ambiguous location (from both urethane and urea groups) in the hard segment. To overcome this problem, perfluoro chain extenders were used in the present study. The high photoemission cross section for fluorine and the precise localization of the fluorine in the hard segment reduce ambiguity in the interpretation of results.

Blackwell et al. suggested that for chain-extended polyurethanes, chain extenders containing an even number of carbons produced polymers that were more phase separated than those containing chain extenders with an odd number of carbons.[20-22] On the basis of such observations a four-carbon fluorine-containing chain extender and a similar five-carbon compound were used in our syntheses of segmented polyurethanes to investigate the carbon-number effect on the surface compositional organization. Two planar aromatic fluorinated chain extenders were also used in syntheses to see whether larger fluorine-containing groups compete with the soft segment for migration to the surface.

It is well-known that the chain length of the soft segment strongly influences the phase separation behavior of segmented polyurethane polymers.[16,17,25,26] Therefore, two series of segmented polyurethanes containing molecular weight 1000 and 2000 poly(tetramethylene glycol) (PTMO) were synthesized to observe the chain length effect. The effect of hard- and soft-segment concentration on the surface structure was investigated by using polymer samples with different hard- and soft-segment ratios. The results obtained from angular-dependent XPS studies indicate that the extent of phase separation in polyurethanes strongly affects the surface structure of the polymers.

Experimental Section

A. Materials. The chain extender 2,2,3,3-tetrafluoro-1,4-butanediol (FB) was prepared by the reduction of diethyl tetrafluorosuccinate (Columbia Organic Chemical Co.) with lithium aluminum hydride in anhydrous diethyl ether.[34] The diol was recrystallized twice from hot benzene solution. It has a melting point of 83 °C (lit. mp ~85 °C). 2,2,3,3,4,4-Hexafluoro-1,5-pentanediol (FP), 1,4-diaminotetrafluorobenzene (TFB), and 4,4′-diaminooctafluorobiphenyl (OFB) were purchased from Columbia Organic Chemical Co. and Aldrich Chemical Co. and recrystallized twice from hot benzene solution. 4,4′-Methylenebis(phenylene isocyanate) (MDI) (The Upjohn Co.) was vacuum-distilled and stored in a refrigerator until used. PTMO's of 1000 and 2000 molecular weight (Quaker Oats Co.) were dehydrated under vacuum at 45–55 °C for 24 h. *N,N*-Dimethylacetamide (DMAc) (Burdick and Jackson) was vacuum-distilled from MDI, and the catalyst, dibutyltin dilaurate (DBDL), was used as received. Highly pure solvents and deionized water were used in all of the processes of preparation to minimize the contamination of the final products.

B. Polymer Synthesis and Purification. 1. Segmented Polymers. The method for preparing the chain-extended polymers was similar to the conventional two-step polyurethane condensation reaction.[35] MDI was dissolved in DMAc in a three-necked, round-bottomed flask under an argon atmosphere. PTMO and the catalyst were subsequently added to the MDI solution at room temperature. The prepolymerization was carried out at 60–70 °C for 1 h. The concentration of the catalyst was 0.2–0.3% by weight of the reactants, and the concentration of reactants in solution was 15–20% (w/v). In the second step, the fluoro chain extender dissolved in DMAc (10% (w/v)) was added drop by drop to the prepolymer solution. For the fluoro aliphatic chain extenders, the chain-extension reaction was continued for 1 h at 60–70 °C. For the fluoro aromatic chain extenders, the reaction proceeded for 2 h at 110–120 °C. The extent of reaction was monitored by observing the disappearance of the isocyanate absorption band (2260–2320 cm^{-1}) using an infrared spectrometer. The polymers were precipitated in water and dried in a vacuum oven at 60 °C for 1 day.

The polymers precipitated in water contained an appreciable content of low molecular weight material, as revealed by gel permeation chromatography (GPC) (Figure 1) and XPS analysis. XPS data suggested that there was an excess of fluorine-containing material on the surface of solvent-cast films. The probable explanation of this observation is that fluorinated oligomers migrate

Chart I

Polyurethane A

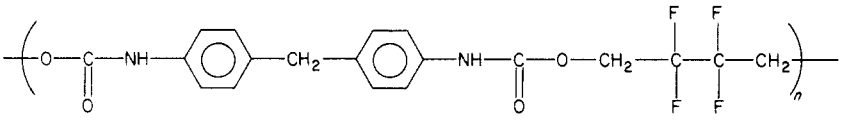

poly(oxycarbonylamino-1,4-phenylenemethylene-1,4-phenyleneaminocarbonyloxy(2,2,3,3-tetrafluorobutane-1,4-diyl))

[poly(2,2,3,3-tetrafluorotetramethylene diphenylmethane dicarbamate)]

Polyurethane B

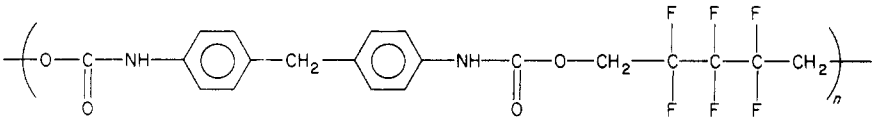

poly(oxycarbonylamino-1,4-phenylenemethylene-1,4-phenyleneaminocarbonyloxy(2,2,3,3,4,4-hexafluoropentane-1,5-diyl))

[poly(2,2,3,3,4,4-hexafluoropentamethylene diphenylmethane dicarbamate)]

Polyurea A

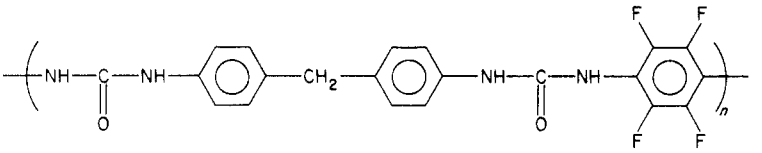

poly(aminocarbonylamino-1,4-phenylenemethylene-1,4-phenyleneaminocarbonylamino-1,4-(2,3,5,6-tetrafluorophenylene))

[poly(tetrafluoro-*p*-phenylene diphenylmethane diurea)]

Polyurea B

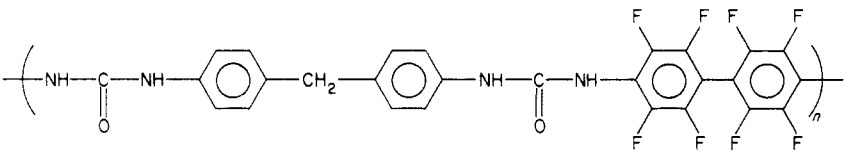

poly(aminocarbonylamino-1,4-phenylenemethylene-1,4-phenyleneaminocarbonylamino(2,2',3,3',5,5',6,6'-octafluorobiphenyl)-4,4'-diyl)

[poly(octafluorobiphenyl diphenylmethane diurea)]

to the surface during solvent evaporation.[31,32] Therefore, all of the polymer samples were redissolved in DMAc and reprecipitated twice in an excess of methanol or a methanol–water mixture (5:1 by volume), depending on the content of hard segment in the polymers. The reprecipitated polymers were filtered, washed thoroughly with methanol, and dried in a vacuum oven at 60 °C for 2 days. The GPC data indicated that the polymers purified by reprecipitation in methanol had reduced levels of low molecular weight components (Figure 1).

The nomenclature used for these polymers is illustrated in the following example: PEU-2000-FP-23 means that the polymer was synthesized by using PTMO of molecular weight 2000 and perfluoropentanediol chain extender (FP) with a feed ratio of 23% by weight (Table I). When a perfluoro aromatic diamine was used as a chain extender, PEUU was used instead of PEU.

2. Hard-Segment Model Polymers. The polyurethanes and polyureas serving as models for the hard segment were prepared from MDI and perfluoro chain extenders. The synthetic method was similar to the previously described, chain-extension reaction scheme. MDI and the perfluoro aliphatic diol (molar ratio 1:1) were dissolved in DMAc (concentration 20% (w/v)) with rapid stirring under an argon atmosphere. After the catalyst, DBDL (0.3–0.4% by weight), was added, and the mixture was stirred at 60–70 °C. After 1 h a highly viscous, clear solution was obtained. The resulting polymer was precipitated in methanol. The precipitated polymer was filtered, thoroughly washed with methanol, and vacuum-dried at 70 °C for 2 days. Both urethane polymers, poly(2,2,3,3-tetrafluorotetramethylene diphenylmethane dicarbamate) (polyurethane A) and poly(2,2,3,3,4,4-hexafluoropentamethylene diphenylmethane dicarbamate) (polyurethane B) were white, brittle solids.

For the synthesis of the hard-segment model polyureas, the reaction temperature was maintained at 115–125 °C for 2 h. In the preparation of poly(tetrafluoro-*p*-phenylene diurea) (polyurea A), there was a small amount of insoluble high polymer precipitated in the reaction solution, which was filtered off with a 0.5-μm Millipore filter. The polymers were precipitated in *n*-butyl acetate, a better solvent than methanol. This solvent helped to remove oligomeric material from the polymer. Polyurea A was a pale yellow, brittle solid, and poly(octafluorobiphenylene diphenylmethane diurea) (polyurea B) was a white, fluffy, and brittle solid. All polymers obtained were further purified by reprecipitation in methanol. The structural formulas for the hard-segment polymers are shown in Chart I.

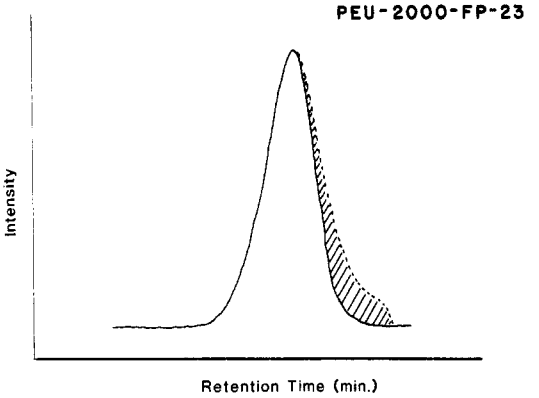

Figure 1. Typical gel permeation chromatograms for unpurified (---) and purified (—) polymer samples. The low molecular weight fraction (shaded area) was removed by reprecipitation in methanol.

C. Polymer Characterization. The bulk characterization of the polymers was carried out by bulk elemental analysis, GPC, and IR. The bulk elemental analysis data (C, H, N, and F) were obtained from Huffman Laboratories (Wheat Ridge, CO). The precision and accuracy for the bulk elemental analyses were within ±0.3% for the four elements in these samples. Bulk oxygen

Table I
Compositions of Segmented Poly(ether urethanes) and Poly(ether urethane ureas) with Various Fluoro Chain Extenders

sample	molar ratio MDI/chain extender/ PTMO	chain extender	mol wt of PTMO	hard segment, wt %	feeded chain extender, wt %	fluorine,[a] atom %	$M_n \times 10^{-3}$
PEU-2000-FB-19	6:5:1	FB	2000	53.6	18.8	4.13	19
PEU-2000-FP-23	6:5:1	FP	2000	56.2	23.2	7.38	30
PEUU-2000-TFB-20	6:5:1	TFB	2000	54.6	20.5	4.36	13
PEUU-2000-OFB-32	6:5:1	OFB	2000	61.1	31.9	7.90	24
PEU-1000-FB-20	4:3:1	FB	1000	59.8	19.5	5.86	21
PEU-1000-FP-24	4:3:1	FP	1000	62.1	24.1	8.49	23
PEU-1000-FP-12	2:1:1	FP	1000	41.6	12.4	3.82	34
PEU-2000-FP-17	4:3:1	FP	2000	45.0	17.4	5.39	31
PEU-2000-FB-6	2:1:1	FB	2000	24.9	6.1	1.41	44
PEU-2000-FP-8	2:1:1	FP	2000	26.3	7.8	1.85	56

[a] The bulk elemental analysis data for purified samples. See text.

analysis data could not be obtained because of the interfering effect of fluorine on the oxygen determination. For our highly purified samples, the oxygen content was calculated from the data obtained. The elemental composition data were renormalized in terms of atom % with respect to the four elements C, O, N, and F. Only the fluorine data are shown in Table I.

The GPC measurements were made to monitor the removal of low molecular weight components in crude polymers (Figure 1). Du Pont Zorbax PSM1000-S and PSM60-S columns were used with a refractive index detector. The flow rate of the DMAc eluent was 1 mL/min. Molecular weights were reported based upon the retention time of polystyrene standards. The apparent number-average molecular weights of purified polymers were in the range 20 000–60 000 (Table I).

The assignments of characteristic IR frequencies in the segmented polyurethanes and poly(urethane ureas) were made by comparison to the IR spectral data for the hard-segment polymers (polyurethanes A and B and polyureas A and B) and other fluoro polymers.[36,37] The IR spectra of FP-chain-extended polymers showed a sharp CF_2 band at 1150 cm^{-1}, the intensity of which depended upon the concentration of chain extender.[36,37] For the FB-chain-extended polymers, the CF_2 band at 1120 cm^{-1}, confirmed from the IR spectrum of polyurethane A, was overlapped with the broad, strong C–O–C bending mode at 1100 cm^{-1} and appeared as a slight shoulder on it. The OFB- and TFB-chain-extended samples showed a characteristic band at 1450–1500 cm^{-1}, which did not appear in the linear fluoro-chain-extended samples. This band, confirmed from the IR spectra of polyureas A and B, may be due to the stretching modes of fluorine-substituted phenyl rings.

D. Surface Characterization by XPS. 1. Sample Preparation. All of the polymer samples for XPS study were centrifugally cast onto clean glass disks of 12-mm diameter at 20–25 °C and 40–50% relative humidity in a class 100 laminar flow hood. The concentration of casting solutions was 1–1.5% (w/v) in dry DMAc, and the spinning rate was 4000 rpm. The solvent was slowly evaporated for 5–6 h in the laminar flow hood before the XPS measurements were made. All coated samples were optically transparent. The films formed are typically 200–800 Å in thickness. Thus, residual DMAc can readily evaporate prior to measurement. The absence of measurable outgassing in the XPS instrument supports the contention that significant levels of residual DMAc are not present during XPS analysis.

2. Instrumentation. All XPS data were collected with a Surface Science Laboratories SSX-100 ESCA spectrometer using an Al Kα X-ray source. A brief description of the characteristics of this spectrometer is found elsewhere.[38,39] The region (spot size) irradiated with monochromatized X-rays was a 600-μm-diameter circle for all samples. The X-ray gun was operated at 10 kV and 12 mA, and the pressure in the analyzer chamber was 10^{-8}–10^{-9} torr. The highest resolution spectra for binding energy (BE) determination were obtained with a 25-eV pass energy with a 30° solid-angle electron collection aperture placed in the electron lens system. Under this experimental condition, the gold $4f_{7/2}$ level at 83.8-eV BE had a full-width half-maximum (FWHM) of 0.9 ± 0.1 eV. All data were processed by using the standard software provided with this instrument. The surface charging that occurred due to the nonconductive nature of the samples was neutralized with 10–15-eV low-energy electrons from an electron flood gun.

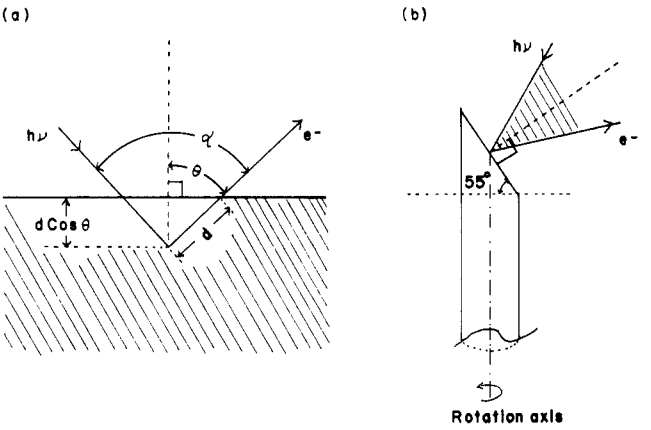

Figure 2. Schematic diagrams of the geometry for XPS angular-dependent experiments.

Table II
Comparison between Bulk Elemental Analysis and XPS Data for Polyurethane A[a]

	% C	% O	% N	% F
theoretical	65.52	13.79	6.89	13.79
bulk elem anal.	65.38	14.20	7.41	13.02
ESCA data	65.31 ± 0.67	13.76 ± 0.47	7.21 ± 0.50	13.71 ± 0.72
sensitivity factor[b]	1.00	2.49	1.68	3.33

[a] Values in atom %. [b] For the SSX-100 ESCA used under the specified conditions.

For the angular-dependent experiments,[40] the 30° solid-angle aperture was replaced with a 6° solid-angle aperture to enhance the depth profile sensitivity. All data collection for the angular-dependent studies was done at 100-eV pass energy. Angular-dependent XPS measurements were made with the experimental geometry shown in Figure 2. The angle between the X-ray source and electron collection optics, α, is fixed at 90° in the SSX-100 ESCA spectrometer. The sample mounting plane, cut elliptically from a cylindrical sample holder, is slanted at 55° with respect to the horizontal plane such that the surface of the sample mounted on it has an angle of 90° relative to the plane of the slits of the fixed-position analyzer. Thus, the angle, θ, between the normal to the sample and the slits in the analyzer can be varied by rotating the sample holder about a rotation axis.

3. Quantitation. The values of sensitivity factors in Table II were used via the software provided with the SSX-100 ESCA system to calculate the atomic percent ratio of four elements in the angular-dependent studies. The sensitivity factors take into account the Scofield photoelectron cross sections,[41] the kinetic energy dependence of the inelastic mean free path of emitted electrons,[42] and the electron kinetic energy dependence of the transmission function,[40,42] $T(E_k)$. The elemental ratios determined

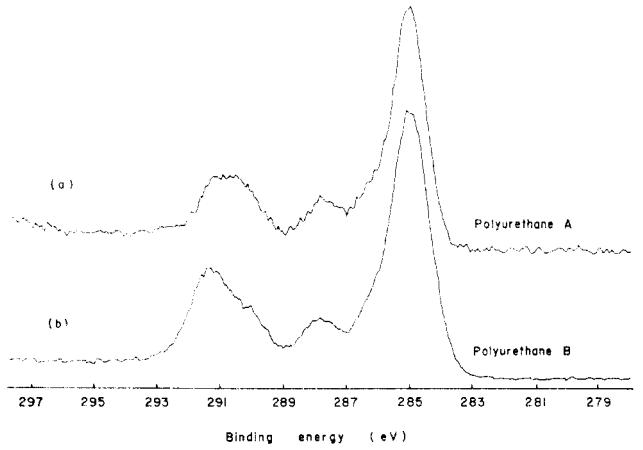

Figure 3. C_{1s} core-level spectra for the fluorine-containing polyurethanes A and B.

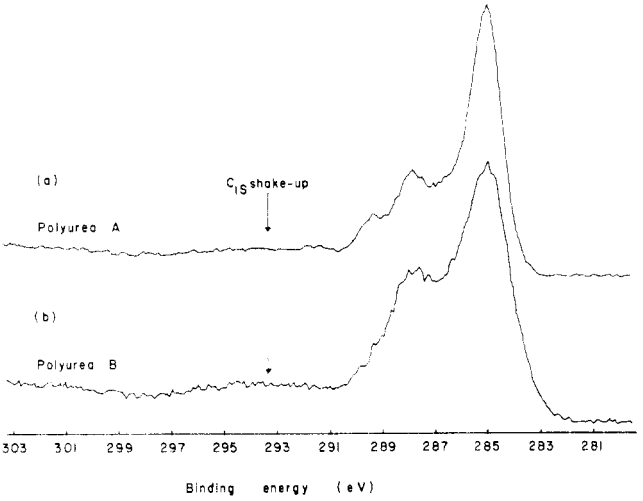

Figure 4. C_{1s} core-level spectra for the fluorine-containing polyureas A and B.

for polyurethane A (M_n = 26 000), using the sensitivity factors in Table II, are within 5% of those obtained with the bulk elemental analysis and are close to the theoretically predicted values. The elemental ratios for smooth films of polyurethane A show no angular dependence; therefore, we can assume that bulk and surface compositions are similar. The other hard-segment polymers gave the same results. Thus, under the specified instrument settings (resolution setting 3 of the SSX-100 instrument was used for all quantitation), good quantitation of data is expected.

Results and Discussion

A. Surface Composition. 1. Model Polymers. In order to interpret the spectral data from segmented fluorine-containing polyurethanes and poly(urethane ureas), it is appropriate to study related hard-segment-rich polymers and soft-segment-rich polymers and to determine their absolute and relative binding energies and relative peak intensities. The C_{1s} core-level spectra of fluorine-containing polyurethanes and polyureas are shown in Figures 3 and 4, respectively. The spectra were resolved with reference to known binding energy data of fluorine- or nitrogen-substituted polymers or model compounds, using the assumption of Gaussian peak shapes. The value of 285.0 eV was used for the binding energy of the C_{1s} core-level photoemission of all peaks indicative of the unsubstituted hydrocarbon.[28,29] The binding energy data (Tables III and IV) give internally consistent values as expected from a consideration of the chemical environment. All binding energy data are reproducible within ±0.2 eV.

Table III
Binding Energy Shifts (Δ (eV)) of C_{1s} Core Levels for Polyurethanes A and B and Polyureas A and B

	polyurethane		polyurea	
	A	B	A	B
(1) C–C, C–H (285.0 eV)	0	0	0	0
(2) C–N	1.2	1.2	1.2	1.2
(3) C–O	2.8	2.9		
(4) C=O	5.1	5.0	4.4	4.2
(5) C–F	6.2	6.2	2.8	2.8
(6) shake-up band			8.0	8.7

Table IV
Binding Energy and Shake-Up Peak Shift Data for F_{1s}, O_{1s}, and N_{1s} Core Levels for Polyurethanes A and B and Polyureas A and B

	F_{1s}	O_{1s}	N_{1s}
polyurethane A	688.4	532.4, 534.4	400.8
	(6.0)[a]	(6.5)	(6.0)
polyurethane B	688.8	532.6, 534.6	401.0
	(5.7)	(7.5)	(7.1)
polyurea A	688.1	532.0	400.7
	(6.2)	(7.6)	(6.2)
polyurea B	688.3	532.1	400.7
	(6.5)	(7.4)	(6.2)

[a] The values in parentheses are shake-up shift values for the corresponding main peaks.

The C_{1s} core-level spectra of polyurethanes consist of well-resolved triplets with an apparent shoulder on the higher binding energy side of the main carbon peak. The broad and symmetric peak at the highest binding energy in Figure 3a actually consists of two peaks of equal area: the higher binding energy peak corresponding to the fluorine-substituted carbon, $-CF_2CF_2-$ (shifted by 6.1 eV from the lowest binding energy peak), and the lower binding energy peak for the urethane-carbonyl carbon, shifted by 5.1 eV. An additional $-CF_2-$ group in the chain (polyurethane B) induces an asymmetric increase of intensity of the higher binding energy peak (Figure 3b). The chemical shift of the fluorine-substituted carbon is comparable to the data reported by Clark et al. for fluoro polymers.[43,44] The assigned chemical shift of 5.1 eV in the urethane-carbonyl (carbamate) carbon was compared to the chemical shift of the carbamate carbon in poly(diphenylmethane tetramethylene dicarbamate). This assigned value is somewhat high compared to that usually observed for this carbon (typically 4.3–4.6 eV), perhaps due to a small inductive effect from the $-CF_2-$ group nearby (three bonds away). Although the highest binding energy peak in polyurethane B shows a distinct peak maximum corresponding to the core ionization of the fluorine-substituted carbons, the more accurate assignment of this binding energy is complicated by the probable presence of a shake-up satellite band shifted by 6.5 eV from the main peak.[27,44] However, the relatively broad and small (~3% or less) contribution of the shake-up band to the high binding energy tail of the peak should have little effect on the binding energy assignment.

The central peak of the spectrum, well resolved from the main peak, was assigned to the core-level photoemission from carbon atoms singly bonded to oxygen in polyurethanes A and B. These carbons have $-CF_2-$ groups at their α positions. Owing to the strong secondary inductive effect of fluorine (one fluorine atom induces a 0.7-eV shift[43,45]), the C_{1s} peak of carbon atoms singly bonded to oxygen is shifted approximately twice that observed in

non-fluorine-containing systems. In such systems, the C–O peak appears as a shoulder or a separately resolved peak ~1.5 eV on the higher binding energy side of the 285.0-eV peak.[45,46] Systems that demonstrate this 1.5-eV binding energy shift include poly(alkyl methacrylates), poly(alkyl acrylates), polyurethanes, and model compounds such as alkyl acetates. As shown in Figure 3, the 285.0-eV carbon peaks both have shoulders on the higher binding energy side. The peak is shifted by about 1.2 eV and is associated with nitrogen singly bonded to carbon on the phenyl ring.[45]

In the fluorine-containing polyureas, an additional tetrafluorophenyl ring induces an increase in the intensity of the central peak in Figure 4a. This peak, shifted by 2.8 eV from the main C_{1s} peak, can be assigned to the C_{1s} peak of the fluorine-substituted carbons on the phenyl ring. The shift value, 2.8 eV, is small compared to the reported value of 3.9 eV for 1,2,4,5-tetrafluorobenzene.[47] This smaller shift could be ascribed to a strong π-electron-donating character of the nitrogens attached to the 3,6-positions on the fluorine-substituted phenyl rings in the polyureas. The highest binding energy side peak, shifted by 4.4 eV, is the urea-carbonyl carbon peak. This urea-carbonyl peak is less shifted than the urethane-carbonyl C_{1s} peak, as expected from the less electronegative nature of nitrogen, but is shifted farther than expected based upon previously reported peak values for ureas.[48] This difference may also be caused by a weak inductive effect through three bonds.

The core-level spectra of F_{1s}, O_{1s}, and N_{1s} for polyurethane B are shown in Figure 5a–c. The spectra for polyurea A are shown in Figure 5a′–c′. The binding energy data for the elements (Table IV) are comparable to reported values.[45]

The O_{1s} spectra show a marked difference between the polyurethane and the polyurea; a symmetrical doublet is produced by the two types of oxygen in the urethane unit. The O_{1s} core electrons of the two carbonyl-type oxygens in the urethane and urea have the same binding energy within experimental error. The slight shoulder of the O_{1s} spectrum of polyurea A may be due to a urethane-ether-type oxygen that probably originated from an impurity in the polymer.

The core-level spectra of all four elements, for all of the polymers under consideration, show definite shake-up features.[27,45] The intensities of shake-up bands accompanying the core ionizations in the polyureas are stronger than those in the polyurethanes. In polyurethanes A and B, the F_{1s} core ionizations are accompanied by weak satellite bands even though the fluorine atom is removed by at least four bonds from the aromatic and carbonyl moieties. In relatively simple aromatic molecules or simple polymeric systems, the satellite peaks accompanying core ionizations are well interpreted in terms of $\pi^* \leftarrow \pi$ excitation transitions.[27,45,49] But, in polymer systems with backbone aromatic functionalities, the interpretation is more complicated because greater delocalization of molecular orbitals is expected, as in the present system of highly conjugated polyureas and polyurethanes.[50]

2. Segmented Polyurethanes and Poly(urethane ureas). Typical C_{1s} core-level spectra of fluorine-containing segmented polyurethanes and poly(urethane ureas) are shown in Figure 6. In the spectrum of PEU-2000-FP-8 (reaction feed ratio, MDI:FP:PTMO = 2:1:1) (Figure 6a), the strong higher binding energy subpeak, shifted 1.4 eV from the main peak, corresponds primarily to the C_{1s} core-level photoemission of carbon singly bonded to oxygen[45,46,48] originating from the soft segment of PTMO. As a first-order approximation, the maximum of the main peak was assigned at 285.0 eV for binding energy referencing. It is apparent from the spectra (Figure 6a–c) that the concentration of hard segment at the polymer surfaces, as inferred from the relative intensity of the small, broad peak at ~291 eV, increases as the soft-segment concentration decreases. The increase in hard-segment concentration results in the broadening of the main doublet peak because of the increase in the ether-type carbon ($-OCH_2CF_2-$) concentration at the surface.

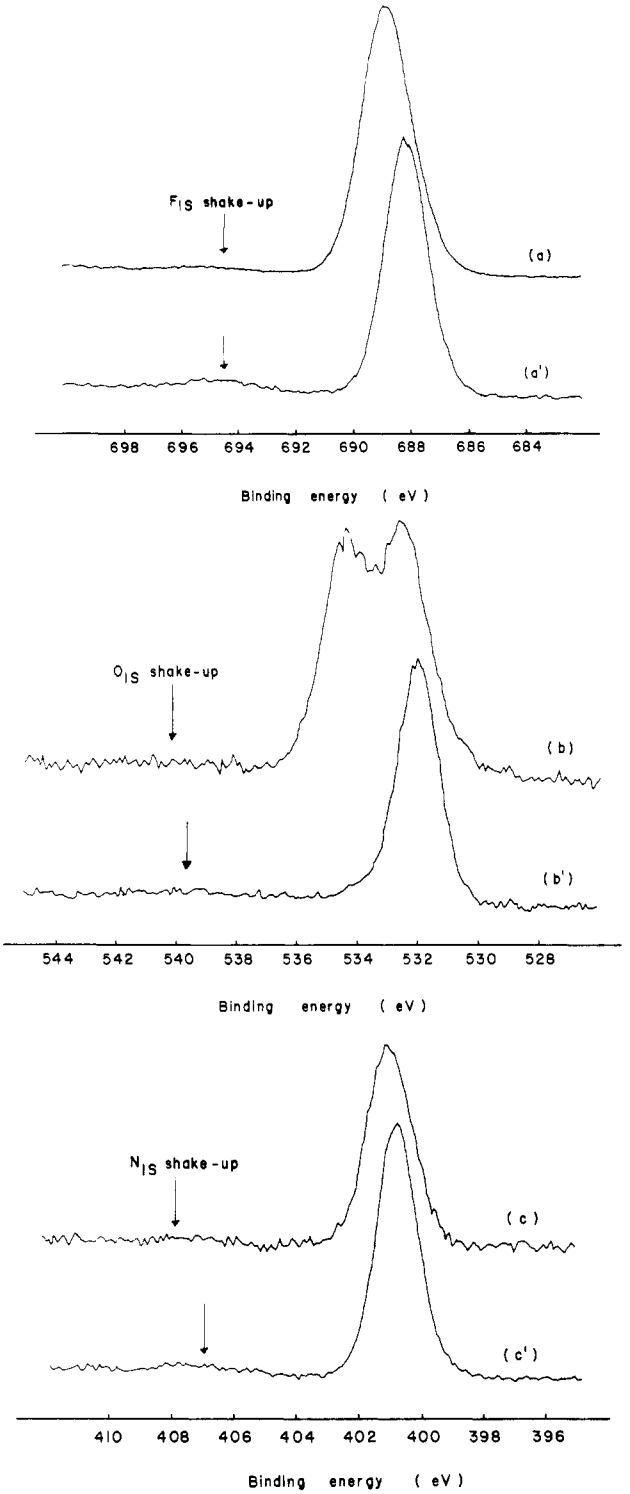

Figure 5. F_{1s}, O_{1s}, and N_{1s} core-level spectra for polyurethane B (a, b, and c, respectively) and polyurea A (a′, b′ and c′, respectively).

In a conventional segmented polyurethane system, both the C_{1s} peak from the urethane-carbonyl carbon and the N_{1s} peak can be used for the quantitative determination of hard-segment concentration at the surface.[31] But there

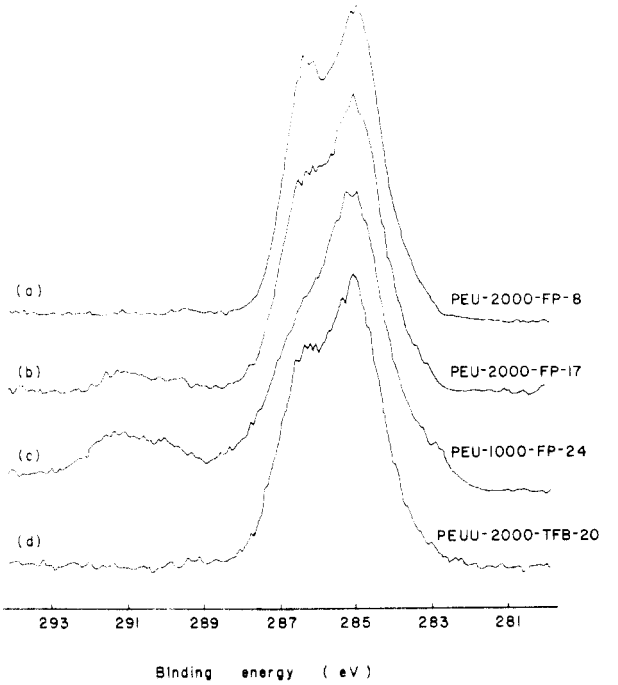

Figure 6. C_{1s} core-level spectra of segmented fluorine-containing polyurethane and poly(urethane urea) polymers.

are two problems that must be considered for this quantitative study. The first problem is that large errors can be introduced in the area determination since the two peaks have small signal intensities. The second consideration is that each peak has two contributions, one derived from the hard segment containing the chain extender and the other from the non-chain-extender hard segment introduced in the prepolymerization step. The latter artifactual contribution to the hard-segment signal may not be a part of the phase-separated hard domains because of the local high concentration of tetramethylene oxide in the soft segment and because of conformational constraints. As the hard-segment content decreases, the potential error is more significant. Therefore, the overall measurement of hard segment using components of the C_{1s} core-level peak or the N_{1s} peak may give ambiguous results in depth profiling studies.

In the fluorine-containing systems described in this work, the use of the F_{1s} signal from only the chain-extender hard segment effectively removes the curve resolution and low sensitivity problems from the data analysis. The F_{1s} signal reflects only the "real" hard segments. Also, the F_{1s} signal has a high photoemission cross section compared to nitrogen.[47] Therefore both the sensitivity and the significance of the angular-dependent depth profiling using the F_{1s} photoemission should be higher than in studies utilizing N_{1s} measurements. These points will be further discussed in the section "Angular-Dependent Studies" (below).

As shown in Figure 6d, no easily resolvable peak indicative of the carbamate carbons is present in the C_{1s} spectrum of a fluorine-containing segmented poly(urethane urea), probably due to the low concentration of this unit. Still, in the case of the segmented poly(urethane ureas), both the F_{1s} and the N_{1s} core levels can be used for depth profiling analysis in the angular-dependent studies because the nitrogen content is twice that of the segmented polyurethanes and the contribution of the nitrogen in the soft segment is reduced.

B. Angular-Dependent Studies. As shown in Figure 2, a variation in the take-off angle, θ, results in a change

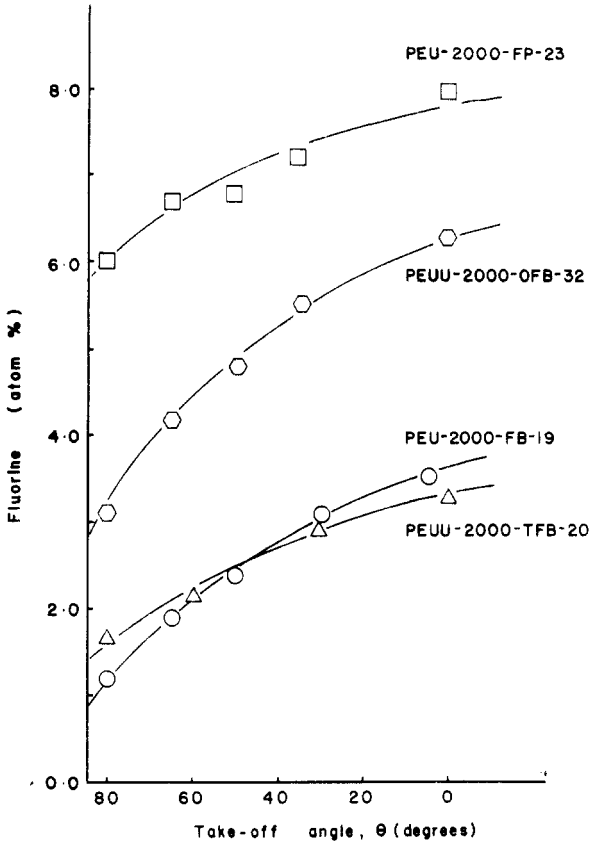

Figure 7. XPS angular dependence of the fluorine signal for segmented polyurethanes and poly(urethane ureas). The feed molar ratio of MDI, chain extender, and PTMO-2000 was 6:5:1 for the four samples.

of the effective sampling depth. The sampling depth ($d \simeq 3\lambda_e$) is defined as the depth from which about 95% of the signal comes and depends on the electron inelastic mean free paths (λ_e) appropriate to photoemitted electrons from the core levels.[45]

Although there is some controversy about the values of λ_e determined for organic and polymeric materials,[51-53] it is thought that the sampling depths are in the range 100 ± 50 Å. Therefore, the effective sampling depth may be changed from ~100 to ~20 Å with the variation in take-off angle from 0° to 80°, and electrons collected at grazing exit angles to the plane of the surface (θ = 80°) will enhance surface features relative to electrons collected normal to the surface (θ = 0°).

Data from angular-dependent XPS studies are difficult to interpret if the surfaces under study are not smooth. Scanning electron micrograph studies confirmed that the specimens used in this work were indeed very smooth.

1. Angular Dependence of Fluorine Content. The angular dependence of the F_{1s} signal is shown in Figure 7 for PEU-2000 and PEUU-2000 samples, chain-extended with FB, FP, TFB, and OFB, respectively; the feed molar ratios for MDI, fluoro chain extender, and PTMO were 6:5:1. All of the percent fluorine data are reproducible within ±5%. For vertically homogeneous homopolymers, relative intensities do not change with take-off angle, θ.[45,53] The data clearly show that the surfaces of the segmented polyurethanes and poly(urethane ureas) have different compositions from the bulk within the uppermost ~100 Å and that the soft segment is most likely richer at the surface than in the bulk. The fluorine content increases monotonically with effective sampling depth and reaches 80–100% of the bulk value (Table V) at the maximum effective sampling depth.

Table V
Comparison of Fluorine Content between Bulk and Surface Compositions

sample	surface, atom % 80°	surface, atom % 0°	bulk,[a] atom %	% F bulk/ % F surface[b]
PEU-2000-FP-23	6.03	8.01	7.38	1.3
PEU-2000-FB-19	1.22	3.53	4.13	2.9
PEUU-2000-OFB-32	3.12	6.28	7.90	2.0
PEUU-2000-TFB-20	1.69	3.29	4.36	2.0
PEU-2000-FP-17	4.52	6.62	5.39	1.4
PEU-2000-FP-8	1.07	1.57	1.85	1.5
PEU-2000-FB-6	0.72	1.34	1.41	1.9
PEU-1000-FP-24	8.73	8.79	8.49	1.0
PEU-1000-FP-12	2.76	3.54	3.82	1.3
PEU-1000-FB-20	4.98	6.43	5.86	1.3

[a] Data from bulk chemical analysis. [b] ESCA data.

The angular-dependent signal intensities for fluorine show different trends as a function of θ, depending on the type of chain extender employed; the PEUU-2000-OFB-32 sample has twice the fluorine content of PEUU-2000-TFB-20 at every effective sampling depth. Considering that the theoretical stoichiometric ratio of the atom % fluorine for the two chain extenders is two and that the fluorine content ratio is also approximately two in the bulk of the two samples (Tables I and V), we suggest that an additional planar phenyl ring in the chain extender has no effect on the surface vertical organization and simply serves to increase the fluorine content at the surface. The similarity of depth profile behavior between the two segmented poly(urethane urea) samples implies that if the fluorine content or hard-segment distribution in the surface region depends on the extent of phase separation of the bulk phase, the bulk phase of the two polymers should have almost the same degree of phase separation and hard-domain sizes. This similarity in phase separation is as expected from the similar planar structures of the two chain-extender molecules. Therefore, an additional fluorine-containing group of similar geometrical (planar) structure has little or no effect on the preferential migration of soft segment to the surface.

In contrast to the planar aromatic chain-extender samples, PEU-2000 samples chain-extended with each of the fluoro aliphatic chain extenders (FP and FB) show a strong variation in the ratio of their fluorine contents as a function of angle. For example, the surface fluorine ratio of PEU-2000-FP-23 and PEU-2000-FB-19 varies from 5.0 at 80° to 2.3 at 0° (Table V). When compared to the bulk ratio value of 1.8, which is slightly higher than the stoichiometric ratio value of 1.5, the high surface ratio value and its large variation with θ indicate that the specimen prepared with hexafluoropentanediol has a larger hard-segment fraction at the surface than the tetrafluorobutanediol sample. Also, the phase separation tendencies in the bulk phase are quite dissimilar for the two chain extenders, as expected from the differences in the angular dependence of the fluorine signals that were observed. Now, let us consider why an additional $-CF_2-$ group in the chain extender induces such a large difference between the surface structures of the two samples.

From X-ray diffraction and conformational analysis studies for poly(MDI/linear aliphatic diol) and the hard segments in MDI/diol/poly(tetramethylene adipate)-based segmented polyurethanes, Blackwell and co-workers suggested that for linear (C_4–C_8) diol chain extenders, the structure is dependent upon whether the diol has an even or odd number of $-CH_2-$ groups.[20-22] The butanediol-chain-extended polymers adopt the lowest energy, fully extended conformations in which, for the chain extender unit $-O(CH_2)_4O-$, all the chain bonds possess trans conformations to allow for effective hydrogen bonding. But, for the pentanediol polymer, two gauche$^+$ bonds are needed in the chain-extender region to satisfactorily explain the shorter fiber-repeat unit compared to that of the butanediol polymer. The presence of these bonds results in nonlinear hydrogen bonding and in a contracted chain conformation compared to the case for even diol polymers. On the basis of these structural analyses, Blackwell et al. suggested that the hard segments of even diol polymers crystallize more easily in the lowest energy, extended conformations and that there is a greater driving force for phase separation in even diol polymers than in odd diol polymers. These suggestions are supported by the work of Critchfield et al. for MDI/2000 M_n poly(caprolactone)-based polyurethanes.[54] Critchfield found that the mechanical properties depend on the linear aliphatic glycol chain extenders (C_2–C_{12}) used. Earlier work by Bonart et al. on small-angle X-ray scattering also showed that 1,4-butanediol-chain-extended polymers are better phase separated than 1,5-pentanediol polymers and that the hard-segment domain size of the former is larger than that of the latter.[19]

Let us consider the case in which H is replaced by F in the chain-extender region. The conformational analysis data in linear low molecular weight perfluorocarbons suggests close resemblance to the conformational energy of hydrocarbon chains.[55] The major difference is that the stability of the trans conformation with respect to the gauche conformation for the fluorocarbon is much higher than that for the hydrocarbon analogue because the fluorocarbon exhibits greater steric repulsion in the gauche state as a consequence of the greater van der Waals radius of fluorine. Among the conformational models of poly(MDI/pentanediol) by Blackwell et al. that are compatible with the observed monomer repeat unit, the conformation of g^+tttg^+ in the $-O(CH_2)_5O-$ unit may be most suitable for the analogue of the hexafluoropentanediol chain-extended sample because the other two models have two gauche bonds in the central atoms (energetically less stable situations in the fluorine-substituted system).[20] Thus, in spite of the small conformational differences that probably exist, we may assume that the fluorine-substituted butanediol and pentanediol analogous hard segments are conformationally similar. From this conformational analogy, it is reasonable to ascribe the observation that perfluoropentanediol (odd diol) samples have a higher fluorine content or hard-segment concentration at the surface than perfluorobutanediol (even diol) samples due to the poor phase separation of the former.[19,20]

The effect of soft-segment molecular weight on surface topography is shown in Figure 8. All of the samples have similar hard-segment concentrations (55–60% by weight) except for PEU-1000-FP-12 (40% by weight). Interestingly, the PEU-1000-FP-24 sample shows no angular dependence while PEU-1000-FP-12 has a slight angular dependence. PEU-1000-FB-20 exhibits an angular dependence, though the dependency is relatively weak compared to its PTMO-2000 counterpart. As shown in Table V, the ratio of the fluorine content at 0° take-off angle to that at 80° take-off angle for PEU-2000-FB-19 is 2.9 while the ratio for PEU-1000-FB-20 is only 1.3. In the FP-chain-extended system, the decrease in the soft-segment molecular weight from 2000 to 1000 produces an increase in the fluorine content or hard-segment concentration at the surface, which eventually approaches the bulk value within the uppermost ~100 Å.

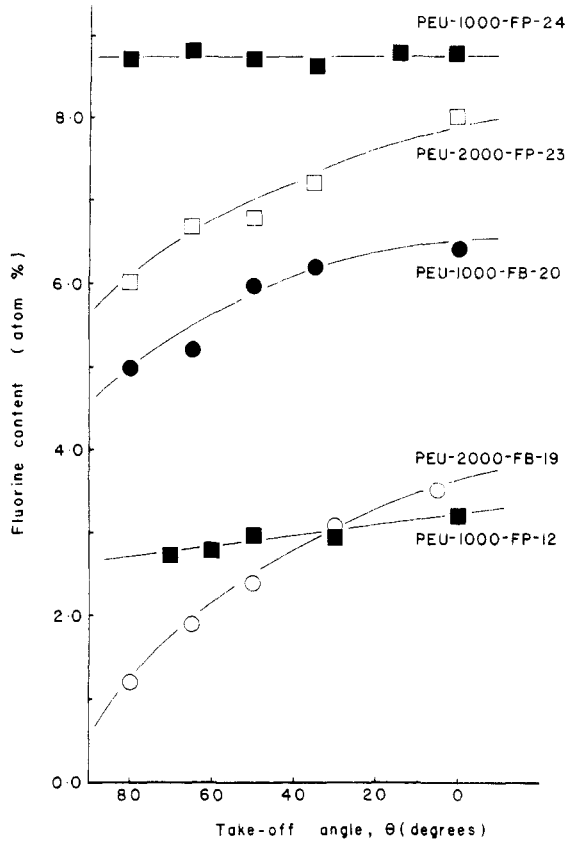

Figure 8. Effect of the soft-segment molecular weight on the fluorine signal XPS angular dependence for segmented polyurethanes. The polymers have the same hard-segment content except for PEU-1000-FP-12. The darkened symbols are for PTMO-1000 samples, and the open symbols, for PTMO-2000 samples.

In bulk property studies which investigate glass transition temperature,[16,25] stress-strain behavior,[17,26] stress hysteresis,[17,25] stress relaxation,[17] and small-angle X-ray scattering[16,25] for non-fluorine-containing segmented poly(urethane ureas) based on 2,4-tolyl diisocyanate (2,4-TDI) or MDI, a soft-segment molecular weight effect is also observed. For the same hard-segment content (30%), the hard domains in the PTMO-1000 sample are more interconnected than the hard domains in the PTMO-2000 sample, and the soft-segment phase of the former contains more solubilized hard segment than that of the latter.[16,17,25,26] The better phase separation of the PTMO-2000 samples might be attributed to the increased thermodynamic incompatibility,[26] resulting from the higher Flory–Huggins interaction parameter (χ)[56] and/or the higher crystallizability[25] of the PTMO-2000 soft segment. This separation is reasonable since a reduced chain length in block copolymers imparts to the system more configurational constraint, thereby inhibiting phase separation.[57]

From the consistent relationship between bulk properties and XPS depth profile data, we can surmise that, along with the "odd diol effect", the decrease in the soft-segment chain length effectively impedes the phase segregation and that the poorer the phase separation, the higher is the concentration of hard segment at the surface. Of course, the interpretation of phase separation from XPS data can be applied only to a relatively pure and fractionated polymer system which has negligible levels of low molecular weight components because the low molecular weight components can migrate to the surface during solvent evaporation.[31,32] Although reasonable arguments have been presented concerning our assumptions on the probable degree of phase separation in the bulk of these polymers, actual measurements have not yet been completed. Such measurements are under way and will be reported in a second paper in this series.

The effects of the bulk composition and the hard-segment block length on the surface compositional organization are illustrated in Figure 9. The values of the surface fluorine content are indicative of the topmost surface (effective sampling depth of ~20 Å). The data points for the PEU-1000-FP samples are on the diagonal line indicating equal concentrations of urethane both at the surface and in the bulk. Thus, an increase in urethane content, accompanied by an increase in hard-segment block length, simply results in the linear and equal increase in fluorine in both regions; i.e., there is no effect on phase separation in the bulk. In addition to the "odd diol" and the soft-segment-length effects on surface compositional behavior, there may be a contribution to the surface structure originating from the multiplicity of blocks and the wide distribution of block lengths. In contrast to copolymers containing long, discrete blocks (e.g., styrene–butadiene di- or triblock copolymers),[14] a segmented polyurethane based on MDI/butanediol/PTMO-1000 of 28% hard-segment content has an interfacial zone equal to one-third of the volume of the hard domain.[23] This zone is much larger than the analogous regions of "long" block copolymers containing well-defined domains. Therefore, in the PEU-1000-FP system where steric factors strongly inhibit domain formation, there is only a straightforward concentration effect on surface topography, as opposed to the more complex effects found in systems such as polystyrene–poly(ethylene oxide) diblock or triblock copolymers.[28,29] Decreasing the factors that inhibit phase separation results in a deviation from the diagonal line as with the PEU-2000-FB samples. In addition, as expected, the soft-segment chain length effect is much larger in FB samples than in FP samples.

For all samples in this study, the concentration of soft segment at the surface is greater than or equal to that in bulk. Thus, it is appropriate to consider the high migration tendency of the soft segment to the surface. The major difference between conventional segmented polyurethanes (or polyureas) and the system in this study is that the hard segment in the present study contains fluorine atoms. The surface fluorine contents of the two aromatic chain-extender samples (Figure 9) are on a collinear line from the origin, and they are linearly proportional to bulk values. This linearity suggests that the similar planar character of the two chain extenders may give them the same conformational "access" to the surface structure. For these planar, aromatic chain extenders, additional fluorines in the chain extender have little effect on the preferential migration tendency of the soft segment under the same conformational constraint conditions. This lack of effect seems reasonable since the concentration of chain extender is relatively small (feed value, 20–30% by weight) and the fluorine atoms are localized in the chain-extender unit of the highly polar hard-segment region (the dipole moment of urethane or urea unit = 3.5–4.5 D[57]). In some block copolymers, lower surface free energy may be a driving force for the enriching of certain components at the surface.[27,28] From the XPS data for our samples showing surface polyether enrichment, we suggest that the less polar soft segment (the dipole moment of the oxide ≃ 1.2–1.5 D[57]) might have a lower surface free energy than the fluorine-containing hard segment. Contact angle studies are under way to gain further insight into the surface energetics of these polymers.

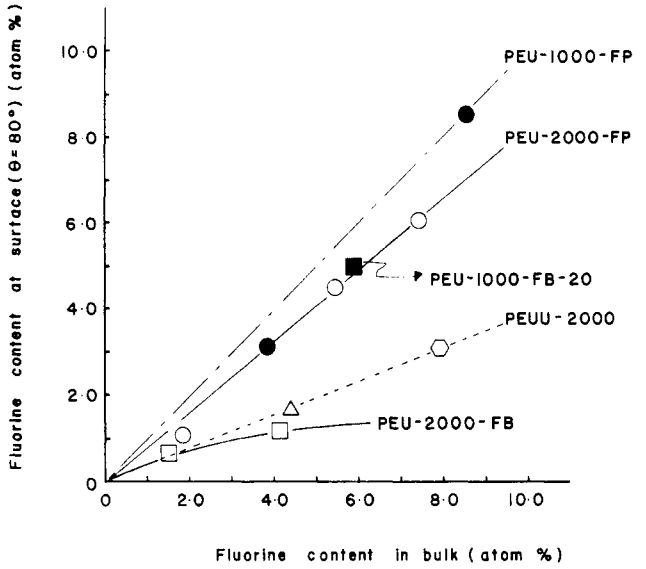

Figure 9. Relationship between the surface concentration of hard segment (measured at $\theta = 80°$) and the bulk composition. The darkened symbols are for PTMO-1000 samples; (○) FP-chain-extended samples; (□) FB-chain-extended samples; (△) TFB-chain-extended polymer; (○) OFB-chain-extended polymer.

2. Angular Dependence of the Nitrogen Signal. Because of the increasing influence of nitrogen that is not in the hard segment as the surface is approached, the nitrogen content data show, for some of the polyurethanes, unexpected fluctuations with respect to the take-off angle. In the low hard-segment samples, PEU-2000-FB-6 and PEU-2000-FP-8 (Figure 10), the functional nitrogen content exhibits a maximum at a 50–40° take-off angle. This maximum is a consequence of the competing relationship between the hard- and soft-segment nitrogens as θ decreases. The PEU-1000-FP-24 sample (Figure 10) exhibits a parallel of the fluorine and nitrogen content with depth. The average-value ratio, F/N, of 2.1 ± 0.1 at the surface is comparable to the ratio value of 2.0 ± 0.1 in the bulk. These results again support the presence of a high degree of mixing of hard and soft segments in the PEU-1000-FP-24 sample.

As previously mentioned, in poly(urethane urea) systems, fluorine and nitrogen can be used as probes for depth analysis, owing to the reduced contribution of the nitrogen in the soft segment. But, when compared to the fluorine depth profile, the nitrogen depth profile still shows some anomalies due to the small fraction of nitrogen in the soft segment as can be seen from the increased curvature at the 60°–40° take-off angle (Figure 10). The two poly(urethane urea) samples PEUU-2000-OFB-32 and PEUU-2000-TFB-20 exhibit the same nitrogen signal angular dependence within experimental error. The ratio of the nitrogen content in the bulk is, for the two samples, 1.1 ± 0.1. These results support the conclusion previously made based upon the fluorine photoemission intensity angular dependence, i.e., that similar surface and bulk compositional structure exists in the two poly(urethane urea) samples.

C. Biomedical Implications. No direct evidence of the existence of discrete domains in the outermost surface layer was obtained from this study. In fact, for polymers expected to be highly phase segregated (e.g., PEU-2000-FB-19), the evidence obtained here suggests that at the surface, the polyether phase "overlayers" the bulk domain structure of the polymer. Thus, only one phase may exist at the outermost surface. For polymers with minimal phase segregation (e.g., PEU-1000-FP-24), the surface and bulk are similar and probably consist of a relatively uniform mixture of hard-segment and soft-segment components.

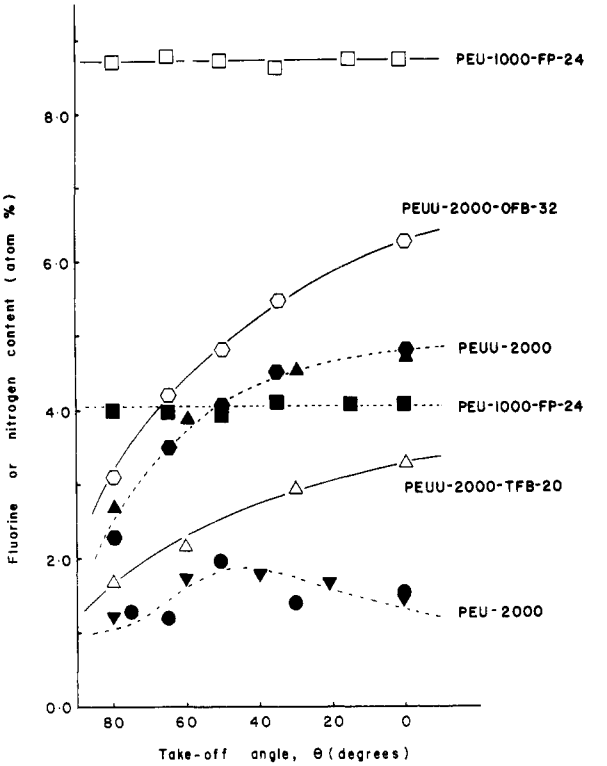

Figure 10. Comparison of the angular dependence of the fluorine and the nitrogen XPS signals. The darkened symbols are for nitrogen content data and the open symbols are for fluorine content data: (△) TFB-chain-extended polymer; (○) OFB-chain-extended polymer; (○) PEU-2000-FP-8 polymer; (▽) PEU-2000-FB-6 polymer.

On the basis of these results, biointeraction studies that attribute unique properties to phase-segregated structures at the surface should be reevaluated. Of course, the surface structure may be substantially rearranged after lengthy contact with aqueous media.[58,59] It is not yet possible to accurately predict how an aqueous interface will alter the surface composition of a phase-separated polymer since both energetic and mobility considerations come into play. Similarly, in block copolymers with one highly crystallizable phase, due to limited chain mobility, both phases might simultaneously exist at the surface.

Conclusions

Utilizing angular-dependent XPS measurements and fluorine labels in polyurethane hard segments, the following conclusions have been drawn concerning the nature of polyurethane surfaces:

1. In fluorine-containing segmented polyurethanes, purified by reprecipitation in methanol to remove low molecular weight material, the odd diol (FP) chain-extended polymers have more hard segment at the surface than the even diol (FB) polymers.

2. A decrease in the chain length of the soft segment has an effect similar to that of using an odd diol in the synthesis, i.e., decreased surface segregation of the soft segment.

3. Under the same conditions of conformational constraint, limited amounts of additional fluorine in the hard segment will not alter the preferential migration of the soft segment to the surface. Thus, steric and conformational factors dominate or overshadow the often-observed ther-

modynamic driving force that attempts to reduce the interfacial energy.

4. The surface compositional organization of segmented polyurethanes or poly(urethane ureas) can be correlated with the bulk structure of these polymers and with the extent of phase separation.

5. The existence of discrete domains on the surface of a polyurethane could not be proven, and, in fact, has been shown to be improbable.

6. Since the surface structure of polyurethanes has been shown to strongly correlate with the biological response to these materials,[1,48] the results obtained here suggest methods to engineer surfaces to exhibit the desired biological performance.

These conclusions were arrived at by making the following refinements to the study of polyurethane surfaces by the angular-dependent XPS technique:

1. All low molecular weight, potentially surface active components were removed.

2. The surfaces were confirmed to be smooth.

3. XPS sensitivity factors were established by using well-defined model compounds that do not exhibit an angular dependence in their XPS-determined elemental ratios.

4. Model compound studies were used to clearly define chemical shifts.

5. Fluorine labels were used to clearly discriminate the location of the hard segment.

Acknowledgment. The experiments described here have been generously supported by N.I.H. Grants HL-25951 and RR-01296 (NESAC/Bio). The assistance of Brien McElroy with the XPS studies is gratefully acknowledged.

Registry No. Polyurethane A (SRU), 100243-86-5; polyurethane A (copolymer), 100297-26-5; polyurethane B (SRU), 100243-87-6; polyurethane B (copolymer), 100297-27-6; polyurea A (SRU), 100243-88-7; polyurea A (copolymer), 100297-28-7; polyurea B (SRU), 100243-89-8; polyurea B (copolymer), 100243-85-4; (MDI)·(PTMO)·(FB) (copolymer), 100243-90-1; (MDI)·(PTMO)·(FP) (copolymer), 100243-91-2; (MDI)·(PTMO)·(TFB) (copolymer), 100243-92-3; (MDI)·(PTMO)·(OFB) (copolymer), 100243-93-4.

References and Notes

(1) Hanson, S. R.; Harker, L. A.; Ratner, B. D.; Hoffman, A. S. In "Biomaterials 1980, Advances in Biomaterials"; Winter, G. D., Gibbons, D. F., Plenk, H., Jr., Eds.; Wiley: Chichester, England, 1982; Vol. 3, pp 519–530.
(2) Hanson, S. R.; Harker, L. A.; Ratner, B. D.; Hoffman, A. S. *J. Lab. Clin. Med.* **1980**, *95* (2), 289.
(3) Ratner, B. D.; Kaul, A. "Polyurethane Surfaces and Interfaces: Implications for Adhesion and Bioadhesion", Abstracts of the Adhesion Society Meeting, Jacksonville, FL, Feb 13–15, 1984.
(4) Hammond, J. S.; Holubke, J. W.; DeVries, J. E.; Dickie, R. A. *Corros. Sci.* **1981**, *239*.
(5) Hoffman, D. M.; Walkup, C. M.; Chiu, I. L. *Ind. Eng. Chem. Prod. Res. Dev.* **1984**, *23*, 572.
(6) Whicher, S. J.; Brash, J. L. In "Physicochemical Aspects of Polymer Surfaces"; Mittal, K. L., Ed.; Plenum Press: New York, 1981; Vol. 2, pp 985–1002.
(7) Okano, T.; Nishiyama, S.; Shinohara, I.; Akaike, T.; Sakurai, Y.; Kataoka, K.; Tsuruta, T. *J. Biomed. Mater. Res.* **1981**, *15* (3), 393.
(8) Kataoka, K.; Okano, T.; Sakurai, Y.; Nishimura, T.; Inque, S.; Watanabe, T.; Maruyama, A.; Tsuruta, T. *Eur. Polym. J.* **1983**, *19* (10/11), 979.
(9) Picha, G. J.; Gibbons, D. F.; Auerbach, R. A. *J. Bioeng.* **1978**, *2*, 301.
(10) Furusawa, K.; Shimura, Y.; Otobe, K.; Atsumi, K. *Kobunshi Ronbunshu* **1977**, *34* (4), 309.
(11) Takahara, A.; Tashita, J.; Kajiyama, T.; Takayanagi, M. *Rep. Prog. Polym. Phys. Jpn.* **1982**, *25*, 841.
(12) Ratner, B. D. In "Surface and Interfacial Aspects of Biomedical Polymers"; Andrade, J. D., Ed.; Plenum: New York, 1985; Vol. 1, pp 373–394.
(13) Hasegawa, H.; Hashimoto, T. *Macromolecules* **1985**, *18*, 589.
(14) Cooper, S. L.; Estes, G. M. "Multiphase Polymers"; American Chemical Society: Washington, DC, 1979; Adv. Chem. Ser. No. 176.
(15) Cooper, S. L.; Tobolsky, A. V. *J. Appl. Polym. Sci.* **1966**, *10*, 1837.
(16) Paik Sung, C. S.; Hu, C. B.; Wu, C. S. *Macromolecules* **1979**, *13*, 111.
(17) Paik Sung, C. S.; Smith, T. W.; Sung, N. H. *Macromolecules* **1980**, *13*, 117.
(18) Bonart, R. *Angew. Makromol. Chem.* **1977**, *58/59*, 259.
(19) Bonart, R.; Morbitzer, L.; Muller, E. H. *J. Macromol. Sci., Phys.* **1974**, *B9* (3), 447.
(20) Blackwell, J.; Nagarajan, M. R.; Hoitink, T. B. *Polymer* **1982**, *23*, 950.
(21) Blackwell, J.; Nagarajan, M. R. *Polymer* **1981**, *22* (2), 202.
(22) Blackwell, J.; Quay, J. R.; Nagarajan, M. R.; Born, L.; Hespe, H. *J. Polym. Sci., Polym. Phys. Ed.* **1984**, *22*, 1247.
(23) Ophir, Z.; Wilkes, G. L. *J. Polym. Sci., Polym. Phys. Ed.* **1980**, *18*, 1469.
(24) Schneider, N. S.; Sung, C. S. P. *Polym. Eng. Sci.* **1977**, *17* (2), 73.
(25) Wang, C. B.; Cooper, S. L. *Macromolecules* **1983**, *16*, 775.
(26) Wilkes, G. L.; Abouzahr, S. *Macromolecules* **1981**, *14*, 456.
(27) Clark, D. T.; Dilks, A.; Peeling, J.; Thomas, H. R. *J. Chem. Soc., Faraday Discuss.* **1975**, *60*, 183.
(28) Thomas, H. R.; O'Malley, J. J. *Macromolecules* **1979**, *12* (2), 323.
(29) O'Malley, J. J.; Thomas, H. R.; Lee, G. M. *Macromolecules* **1979**, *12*, 996.
(30) Fadley, C. S. *Prog. Solid State Chem.* **1976**, *11*, 265.
(31) Hu, C. B.; Sung, C. S. P. *Polym. Prepr., Am. Chem. Soc., Div. Polym. Chem.* **1980**, *21* (1), 156.
(32) Ratner, B. D. In "Physicochemical Aspects of Polymer Surfaces"; Mittal, K. L., Ed.; Plenum: New York, 1983; Vol. 2, pp 969–983.
(33) Ratner, B. D. Proceedings, IUPAC 28th Macromolecular Symposium, July 12–16, 1982, Amherst, MA, p 677.
(34) McBee, E. T.; Marzluff, W. F.; Pierce, O. R. *J. Am. Chem. Soc.* **1952**, *74*, 444.
(35) Saunders, J. H.; Frisch, K. C. "Polyurethanes: Chemistry and Technology. Part 1. Chemistry"; Interscience: New York, 1962.
(36) Hollander, J.; Trischler, F. D.; Gosnell, R. B. *J. Polym. Sci., Part A-1* **1967**, *5*, 2757.
(37) Brown, R. G. *J. Chem. Phys.* **1964**, *40* (10), 2900.
(38) Wagner, C. D.; Joshi, A. *Surf. Interface Anal.* **1984**, *6* (5), 215.
(39) Kelly, M. A. *Res. Dev.* **1984**, *26* (1), 80.
(40) Fadley, C. S.; Baird, R. J.; Siekhaus, W.; Novakov, T.; Bergstrom, S. A. L. *J. Electron Spectrosc. Relat. Phenom.* **1974**, *4*, 93.
(41) Scofield, J. H. *J. Electron. Spectrosc. Relat. Phenom.* **1976**, *8*, 129.
(42) Proctor, A.; Hercules, D. M. *Appl. Spectrosc.* **1984**, *38* (4), 505.
(43) Clark, D. T.; Feast, W. J.; Kilcast, D.; Musgrave, W. K. R. *J. Polym. Sci., Polym. Chem. Ed.* **1973**, *11*, 389.
(44) Clark, D. T.; Thomas, H. R. *J. Polym. Sci., Polym. Chem. Ed.* **1978**, *16*, 791.
(45) Dilks, A. In "Electron Spectroscopy: Theory, Techniques, and Applications"; Baker, A. D., Brundle, C. R., Eds.; Academic Press: London, 1981; Vol. 4, pp 277–359.
(46) Clark, D. T.; Thomas, H. R. *J. Polym. Sci., Polym. Chem. Ed.* **1976**, *14*, 1671.
(47) Clark, D. T.; Kilcast, D.; Adams, D. B.; Musgrave, W. K. R. *J. Electron Spectrosc. Relat. Phenom.* **1972/1973**, *1*, 227.
(48) Ratner, B. D. In "Photon, Electron, and Ion Probes of Polymer Structure and Properties"; Dwight, D. W., Fabish, T. J., Thomas, H. R., Eds.; American Chemical Society: Washington, DC, 1981; ACS Symp. Ser. No. 162, pp 371–382.
(49) Chambers, S. A.; Thomas, T. D. *J. Chem. Phys.* **1977**, *67*, 2596.
(50) Gardella, J. A., Jr.; Chin, R. L.; Ferguson, S. A.; Farrow, M. M. *J. Electron Spectrosc. Relat. Phenom.* **1984**, *34*, 97.
(51) Brundle, C. R.; Hopster, H.; Swalen, J. D. *J. Chem. Phys.* **1979**, *70* (11), 5190.
(52) Cadman, P.; Gossedge, G.; Scott, J. D. *J. Electron Spectrosc. Relat. Phenom.* **1978**, *13*, 1.
(53) Clark, D. T.; Thomas, H. R. *J. Polym. Sci., Polym. Chem. Ed.* **1977**, *15*, 2843.
(54) Critchfield, F. E.; Koleske, J. V.; Magnus, G.; Dodd, J. L. *J. Elastoplast.* **1972**, *4*, 22.
(55) Flory, P. J. "Statistical Mechanics of Chain Molecules"; Interscience: New York, 1969.
(56) Flory, P. J. In "Principles of Polymer Chemistry"; Cornell University Press: Ithaca, NY, 1953; pp 576–594.

(57) Olabisi, O.; Robeson, L. M.; Shaw, M. T. "Polymer–Polymer Miscibility"; Academic Press: New York, 1979.
(58) Gregonis, D. E.; Hsu, R.; Buerger, D. E.; Smith, L. M.; Andrade, J. D. In "Macromolecular Solutions"; Seymour, R. B., Stahl, G. A., Eds.; Pergamon Press: New York, 1982; pp 120–133.
(59) Ratner, B. D.; Weathersby, P. K.; Hoffman, A. S.; Kelly, M. A.; Scharpen, L. H. *J. Appl. Polym. Sci.* 1978, *22*, 643.

X-ray Evidence of an α-Helical Coiled Coil in Poly(γ-dodecyl L-glutamate)

Junji Watanabe* and Hirobumi Ono

Department of Polymer Chemistry, Tokyo Institute of Technology, Ookayama, Meguro-ku, Tokyo, 152 Japan. *Received June 19, 1985*

ABSTRACT: The X-ray diagram of an as-cast film of α-helical poly(γ-dodecyl L-glutamate) displays several striking features: a strong 5.14-Å meridional reflection and a near-equatorial layer line located $^1/_{90}$ Å^{-1} from the equator. These features cannot be accounted for by a simple α-helical conformation but require an α-helical coiled coil. Moreover, the two-chain hexagonal unit net and the assignment of the near-equatorial line to the second layer ($l = 2$) can only be explained by a two-strand structure. These data provide the first X-ray evidence for a coiled-coil structure in a homopolypeptide in which the structure is not stabilized by amphipathic interactions due to a particular sequence of repeating units. From the intensity distribution of the equatorial reflections the radius of the coiled coil is about 5.6 Å. A possible model is described in which the coiled coil consists of two close-packed α-helices with the side chains mainly on the outer surface.

Introduction

The α-helical model accounts satisfactorily for the X-ray diffraction pattern of synthetic polypeptides in the α-form. However, in its simplest form it does not account for the 5.15-Å meridional reflection obtained from the keratin–myosin–epidermin–fibrinogen groups of fibrous α-proteins.[1] Crick[2] and Pauling and Corey[3] independently suggested that this reflection could arise if the axes of the α-helices were distorted to form a long-pitch helix. The resulting conformation was termed a coiled coil.

Pauling and Corey[3] proposed that the distortion arises from the formation of hydrogen bonds of slightly different lengths due to the repeating sequence. A more plausible explanation was offered by Crick,[4] who suggested that supercoiling of two or three α-helices might be stabilized by a regular interlocking of the side chains. Figure 1a represents a radial projection of two α-helices in which the side chains (considered as "knobs") are represented as open and filled circles for the two helices. Crick[4] pointed out that "knob into hole" packing could be achieved over the entire chain length if the chains coiled about each other, as shown in Figure 1b, with the axes of the helices mutually inclined at an appropriate angle α. He derived the structure factor for the following model. The curved α-helix is termed the minor α-helix, and r_j' is the distance of the jth atom from the axis of the minor helix. The more gradual helix traced by the axis of the minor α-helix is termed the major helix. It has radius r_0 and repeat distance C in the z direction. The major helix makes N_0 turns and the minor helix N_1 turns in its own frame, and there are M equally spaced jth atoms in that repeat distance. The values of C, N_0, N_1, and M are 186 Å, 1, 36, and 128, respectively. Denoting the cylindrical coordinates in reciprocal space as R, Ψ, and Z, one may write the structure factor as

$$F(R,\Psi,Z) = F(R,\Psi,l/C) = \sum_p\sum_q\sum_s\sum_j J_p(2\pi R r_0) f_j J_q(2\pi R r_j') J_s\{2\pi(l/C) r_j' \sin\alpha\} \times \exp\{i[p(\pi/2 - \psi_j + \Psi) + q(\pi/2 + \psi_j - \Psi) + s\pi + 2\pi l z_j/C]\} \quad (1)$$

Here f_j is the scattering factor of the jth atom, $J_n(X)$ is the nth-order Bessel function of X, and r_j', ψ_j, and z_j are cylindrical coordinates in real space. The structure factor is nonzero only on layer lines l that satisfy the condition

$$p + 35q + 36s = l + 126m \quad (2)$$

where p, q, s, and m can take integer values. These relations explain the meridional reflection at about 5.15 Å and the strong near-equatorial streak seen in the X-ray patterns of fibrous proteins,[6-9] while neither of these features is expected for straight α-helices.

Crick also suggested[4] that the primary structure stabilizes supercoiling. Elucidation[10-15] of the primary structure of tropomyosin has clarified this relationship. In particular, sequence analysis[10-13] of the tropomyosin chain from rabbit skeletal muscle showed that hydrophobic residues occur at intervals of seven residues. This sequence produces a densely packed hydrophobic region between the two helices, while the longer charged groups (such as arginine, lysine, and glutamic acid) are located on the surface of the coiled coil and are responsible for the solubility and interaction properties. In contrast, Parry and Suzuki[16] concluded from potential energy calculations of poly(L-alanine) that coiled coils are generally more stable than the corresponding single helices. This suggests that no particular repeating sequence of residues is necessary to stabilize the coiled coil. However, there has been no report of synthetic polypeptides in a coiled-coil conformation. They suggested that this may be due to large voids in the coiled-coil structure which can only be filled with a suitable solvent. Some features of the X-ray diffraction pattern expected for coiled coils have been observed for the concentrated phase of poly(γ-benzyl L-glutamate) in *N*,*N*-dimethylformamide.[9,17,18] However, the α-helices in this "complex phase" are straight, and the long-period helix is due to the regular arrangement of the terminal benzyl groups.[17,18] Watanabe et al.[19] confirmed that the benzene rings are cooperatively stacked both in the "complex phase" and in the dried film. This appears to be a stable arrangement, since many other examples of such a face-to-face stacking of benzene rings have been reported.[20-23]

This paper presents the first X-ray evidence for coiled coils in a synthetic homopolypeptide, poly(γ-dodecyl L-glutamate) (PDoDLG), having the following repeating unit

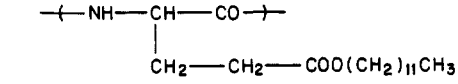

0024-9297/86/2219-1079$01.50/0